Highly efficient broadband polarization retarders and tunable polarization filters made of composite stacks of ordinary wave plates

E. St. Dimova,[1,*] S. S. Ivanov,[2] G. St. Popkirov,[3] and N. V. Vitanov[2]

[1]*Institute of Solid State Physics, BAS, 72 Tzarigradsko Chaussée Blvd., 1784 Sofia, Bulgaria*
[2]*Department of Physics, St. Kliment Ohridski University of Sofia, 5 James Bourchier Blvd., 1164 Sofia, Bulgaria*
[3]*Central Laboratory for Solar Energy and New Energy Sources, BAS, 72 Tzarigradsko Chaussée Blvd., 1784 Sofia, Bulgaria*
**Corresponding author: edimova@issp.bas.bg*

Received December 13, 2013; revised February 28, 2014; accepted March 6, 2014;
posted March 14, 2014 (Doc. ID 201632); published April 8, 2014

By using the formal analogy between the evolution of the state vector in quantum mechanics and the Jones vector in polarization optics, we construct and demonstrate experimentally efficient broadband half-wave polarization retarders and tunable narrowband polarization filters. Both the broadband retarders and the filters are constructed by the same set of stacked standard multiorder optical wave plates (WPs) rotated at different angles with respect to their fast polarization axes: for a certain set of angles this device behaves as a broadband polarization retarder, while for another set of angles it turns into a narrowband polarization filter. We demonstrate that the transmission profile of our filter can be centered around any desired wavelength in a certain vicinity of the design wavelength of the WPs solely by selecting appropriate rotation angles.

OCIS codes: (260.5430) Polarization; (260.1440) Birefringence; (230.5440) Polarization-selective devices; (230.7408) Wavelength filtering devices; (220.4830) Systems design; (220.4610) Optical fabrication.
http://dx.doi.org/10.1364/JOSAA.31.000952

1. INTRODUCTION

Optical polarization retarders have countless applications in physical experiments. Retarders are optical plates, made of birefringent material, that possess two orthogonal axes—ordinary and extraordinary—with different refractive indices, n_o and n_e. Light of wavelength λ passed orthogonally through a retarder of thickness L experiences a retardation (phase shift) $\varphi = 2\pi L(n_e - n_o)/\lambda$. Common types of wave plates (WPs) are half-wave plates (HWPs) with retardation $\varphi = (m+1)\pi$ and quarter-wave plates (QWPs) with $\varphi = (m+1/2)\pi$, $(m = 0, 1, 2, \ldots)$. The QWPs and HWPs can be zero-order $(m = 0)$ or multiorder $(m > 0)$. Because φ depends on λ, the retarders exhibit wavelength dispersion, and therefore QWPs and HWPs are produced with a specified design wavelength. Applications, e.g., in terahertz time-domain spectroscopy [1,2] and in microwave polarimetry [3–5], often demand a wider wavelength range of nearly constant phase retardation.

Achromatic [or broadband (BB)] retarders were first proposed by West and Makas [6] by combining two or more plates with different birefringence, whereby one of the plates is rotated to a specified angle. Destriau and Prouteau [7] used two WPs of the same material but with different thicknesses and axis angles. Pancharatnam used three plates to construct half-wave [8] and quarter-wave [9] BB retarders. Harris *et al.* proposed achromatic QWPs with 6 [10] and 10 [11] stacked identical zero-order QWPs rotated at different angles, optimized to reduce the wavelength dispersion over an extended range. Alternatively, for some applications tunable phase retardation plates can be used. Polarization retarders can be made tunable either by tilting the WPs by a specified angle (Alphalas GmbH, Göttingen) or electrically, by changing the birefringent optical path length using a twisted nematic liquid crystal phase retarder [12,13].

Birefringent phase retarders have also been used to construct narrowband (NB) optical filters. The Lyot [14,15] and Šolc filters [14,16,17] are built using stacks of retarders and polarizers. The possibility of obtaining very NB transmission filters for applications, e.g., solar imaging at specific wavelengths, was also demonstrated [18,19].

Electrically tunable polarization optical filters based on the Lyot filter scheme, using the birefringent effect of electrically controlled liquid crystalline layers instead of solid retarders, have been investigated [20–25] and are already commercially available. Due to the use of polarizers and the limited transmission of liquid crystals, however, the overall peak transmission of filters using a higher number of polarizers and/or liquid crystal elements is relatively poor.

Stacked composite plates are mathematically equivalent to composite pulses in quantum physics, which have been widely used in nuclear magnetic resonance [26] and, recently, in quantum optics [27,28]. This similarity stems from the formal analogy between the Schrödinger equation for a two-state quantum system and the equation for the evolution of the Jones polarization vector [29]. It has been used by Ardavan [30], who proposed using the BB and NB composite pulses of Wimperis [31] to design BB and NB WPs. In a recent work [32], the analogy between the polarization Jones vector and the quantum state vector was used to propose a calculation method for deriving the twisting angles of a stack of retarders

with arbitrarily accurate BB polarization retarders, which promise to deliver very high polarization conversion fidelity in an arbitrarily broad range of wavelengths.

In this paper, we follow the theoretical proposal of Ivanov *et al.* [32] to design and demonstrate experimentally stacked composite plates, which, when rotated at specific angles, act as either BB half-wave retarders or tunable NB filters. In contrast to the earlier demonstration by Peters *et al.* [33], here we use the more flexible single-pass setup rather than the double-pass setup used there. Moreover, we use multiple-order WPs, which are cheaper and easier to produce, and are therefore advantageous for practical reasons. We also use a lamp as a light source, rather than lasers as used in Ref. [33], which allows us to obtain more detailed transmission profiles in a wider wavelength range. Furthermore, the developed model shows how to *tune* the NB filter to *any* desired wavelength (other than the design wavelength λ_0) by merely selecting suitable rotation angles.

In Section 2, we present the theoretical method used to design our polarization BB retarders and NB filters. The experimental apparatus is described in details in Section 3. In Section 4, we show the measured transmittance spectra of our composite filters and BB retarders. In this section, we also show how to tune the central wavelength of the NB filters by simply selecting suitable rotation angles. In Section 5, we present the conclusions.

2. THEORY AND NUMERICAL CALCULATIONS

Here we will summarize the basic theory of composite optical retarders. In the Jones calculus [29], a single birefringent retarder is described by the matrix

$$\mathbf{J}_\alpha(\varphi) = R(-\alpha)\begin{bmatrix} e^{i\varphi/2} & 0 \\ 0 & e^{-i\varphi/2} \end{bmatrix} R(\alpha), \tag{1}$$

where

$$R(\alpha) = \begin{bmatrix} \cos\alpha & \sin\alpha \\ -\sin\alpha & \cos\alpha \end{bmatrix}. \tag{2}$$

We use the linear polarization basis, a pair of orthogonal polarization vectors, where α is the rotation angle of the retarder's optical axis and $\varphi = \varphi(\lambda)$ is the retardation accumulated between the ordinary and the extraordinary rays passing through the retarder. A stack of N retarders is described by the composite Jones matrix

$$\mathbf{J}^{(N)}(\Phi) = \mathbf{J}_{\alpha_N}(\varphi_N)\mathbf{J}_{\alpha_{N-1}}(\varphi_{N-1})\cdots\mathbf{J}_{\alpha_1}(\varphi_1), \tag{3}$$

where the light passes through the plates described by $\mathbf{J}_{\alpha_j}(\varphi_j)$ in the order of ascending index j, i.e., from right to left, and Φ is the overall composite retardation. For the sake of brevity, we denote $\mathbf{J}^{(N)}(\Phi) = \mathbf{J}$. For practical purposes we take all plates to be QWPs (Q) with respect to the design wavelength λ_0. Thus we set $\varphi_j = \varphi_0$, where $\varphi_0 = \pi/2$ for λ_0. This allows us to use commercially available standard WPs.

We thereby assume the following configuration of N plates, each rotated at an angle α_j (see Fig. 1):

$$\mathrm{Q}_{\alpha_1}\mathrm{Q}_{\alpha_2}\cdots\mathrm{Q}_{\alpha_{n-1}}\mathrm{Q}_{\alpha_N}. \tag{4}$$

The overall composite retardation is $\Phi = 2\cos^{-1}\mathrm{Re}\,J_{11}$. The element J_{11} shows the fraction of light intensity that survives when light of a particular polarization is passed through the filter. The retardation profile is symmetric relative to the target retardation $\Phi = \pi$, i.e., $\Phi(\varphi) = \Phi(2\pi - \varphi)$.

By varying the N rotation angles α_j, we obtain different half-wave composite BB retarders and NB filters.

For *BB retarders* the angles α_j satisfy

$$\max(|\Phi(\varphi)/\pi - 1|^2) \le \epsilon, \qquad \varphi \in [\varphi_{\min}, \pi - \varphi_{\min}]. \tag{5}$$

This guarantees that there is a range of single plate retardations between $\varphi_{\min}$ and $\pi - \varphi_{\min}$ (with $\varphi = \pi/2$ corresponding to λ_0), where the composite retardation Φ remains close to π. We determine numerically those angles α_j that minimize $\varphi_{\min}$, giving the broadest possible range of high-quality retardation.

On the contrary, an *NB filter* must transmit only a small spectral region around λ_0. This imposes the following relation on the angles α_j:

$$\max(|J_{12}|^2) \le \epsilon, \qquad \varphi \in [0, \varphi_{\max}]\cup[\pi - \varphi_{\max}, \pi], \tag{6}$$

where $|J_{12}|^2$ represents the filter's intensity transmittance from horizontal to vertical polarization, as known from Jones calculus. We seek those angles α_j that maximize $\varphi_{\max}$, thereby giving the narrowest possible transmission window around $\pi/2$. Outside this window the transmission is maintained below ϵ. For both the BB and NB retarders we choose $\epsilon = 1\%$.

We set the optical axes of the composite retarders and filters at angle 0° by setting $|J_{12}| = 1$ at $\varphi = \pi/2$. This imposes an additional constraint on the angles α_j (cf. Fig. 1), thereby leaving $N - 1$ angles α_j free to vary.

The more angles we can vary, the easier it is to fulfill Eqs. (5) and (6). Therefore, longer sequences [Eq. (4)] of a larger number N of constituent WPs provide larger bandwidths of the broadband retarders or smaller bandwidths for the NB filters.

It is remarkable that we can *tune* the wavelength of the filter, i.e., we can center the transmission window at a wavelength λ' other than the design wavelength of the single plate λ_0, just by varying the values of the rotation angles α_i. The latter are obtained from Eq. (6), where now an offset in the argument of J_{12} is introduced: $J_{12}(\varphi) \to J_{12}(\varphi')$. Here φ' corresponds to the desired new wavelength λ': $\varphi' = 2\pi L(n_e - n_o)/\lambda'$.

For the numerical optimization we use Newton's gradient-based method. Numerous solutions to Eqs. (5) and (6) exist depending on the values of $\varphi_{\min}$ or $\varphi_{\max}$. To determine the optimal solutions, we gradually decrease $\varphi_{\min}$ or increase $\varphi_{\max}$,

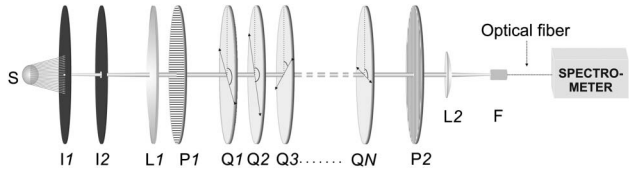

Fig. 1. Experimental setup. The source S, irises I_1 and I_2, lens L_1, and polarizer P_1 form a collimated beam of white polarized light. Polarizer P_2 and lens L_2 focus the beam of output light onto the entrance F of an optical fiber connected to a spectrometer. The composite retarders and filters are constructed by a stack of multiple-order QWPs (Q_n).

until we reach the least $\varphi_{\min}$ or the largest $\varphi_{\max}$ that still satisfies Eq. (5) or (6). Because we use a local optimization algorithm, we iteratively pick the initial parameter values using a Monte Carlo scheme. Although the calculations are made for zero-order plates ($m = 0$), they are valid for multiorder plates too, as the matrix $J_\alpha(\varphi)$ and the ensuing matrix $J^{(N)}(\Phi)$ are periodical in the retardation φ.

The calculated results for the rotation angles α_j of the optical axes of the individual plates for several composite sequences are given in the captions of the figures.

3. EXPERIMENT

We have tested experimentally the calculated BB retarders and NB filters by using the setup shown in Fig. 1. A 10 W Halogen–Bellaphot (Osram) lamp with a DC power supply was used as a source of white light. A collimated light beam was made by using a variable iris I_1 with an aperture less than 0.5 mm positioned at the focus of a plano–convex lens L_1 ($f = 150$ mm). A second iris diaphragm I_2 was used to avoid the outer rings of the beam pattern. The diameter of the beam, measured at a distance of 2 m, was about 2 mm. The light beam was polarized in the horizontal plane by a linear polarizer P_1. A second polarizer P_2 was placed at a distance of 0.7 m and served as an analyzer during the experiments. Both polarizers (Glan–Tayler, 210–1100 nm) were borrowed from a Lambda-950 spectrometer. A second plano–convex lens L_2 ($f = 20$ mm) and a two-axis micropositioner were used to focus the light beam onto the optical fiber entrance F connected to a grating monochromator (model AvaSpec-2048 with controlling software AvaSoft 7.5). Multiorder QWPs (WPMQ10M-780, Thorlabs) were used to build the composite retarders as described above. At the wavelength 780 nm the multiorder QWPs are designed to be 11.25 waves, while at 765 nm they work as HWPs. Each WP (aperture of 1″) was assembled onto a separate RSP1 (Thorlabs) rotation mount. The optical axes of all the WPs were determined with an accuracy of 1°. With the used light source and monochromator, we could obtain reliable spectral transmission data in the range of 400–830 nm.

The composite retarders were assembled as a set of multiorder WPs, each of them rotated at specific angles provided by the calculations, as described above. The WPs were slightly tilted [33] to reduce unwanted reflections. We used a single beam spectrometer, and thus all experiments started with the measurement of the dark and reference spectra. The dark spectrum, taken with the light path blocked, is further automatically used to correct for hardware offsets. The reference spectrum is usually taken with the light source on and a blank sample instead of the sample under test. In our case, however, we have measured the transmission spectrum of the already assembled composite retarder, but the axes of the polarizer P_1 and the analyzer P_2 and the fast axis of the single WPs were all set parallel. The measured light spectrum was used as a reference for the subsequent measurements, with the waveplates rotated at their respective theoretically calculated angles α_j and the analyzer P_2 set to 90°. The transmission spectrum of the so-obtained composite retarder was recorded and scaled to the reference spectrum. The unavoidable losses due to reflections and absorptions from any single waveplate were thereby taken into account. The obtained spectrum predominantly depends on the effective retardance of the composite retarder.

When the composite half-wave retarder was built using QWPs, the measured transmission spectra for both BB and NB retarders were compared with the spectrum of two QWPs assembled to act as a single HWP. In the cases when the WPMQ10M-780 WPs were used as HWPs at 765 nm, the measured transmission spectrum of a single WP was used to demonstrate the broadening or narrowing effect.

According to the theoretical model, there are many suitable sets of angles for the composite retarders. In all cases we have tested experimentally up to 10 different sets of angles for each retarder type, but here, for the sake of brevity, we present only the representative results.

4. EXPERIMENTAL RESULTS

A. Broadband Polarization Retarders

In this section we will demonstrate that using the calculation method described above, composite half-wave retarders with an enhanced wavelength range can be assembled using a set of multiorder WPs. The design wavelength of the used multiorder (11.25 wave) QWPs (WPMQ10M-780) is 780 nm. These WPs could also be used at 765 nm as HWPs (cf. the data sheet of WPMQ10M-780, Thorlabs). We will demonstrate here how these commercial QWPs can be used to construct a composite BB HWP for both the designed wavelength 780 and 765 nm.

First, a composite HWP was made using six multiorder QWPs (WPMQ10M-780). The QWPs were twisted to the respective angles listed in the caption of Fig. 2. Figure 2 shows the transmittance curve. For comparison, the transmittance spectrum of an HWP built using two QWPs with parallel axes is shown too. The significant wavelength range broadening yielded by the composite HWP retarder is evident: the width of the 90%-efficiency range is nearly tripled.

In a second experiment, a BB HWP for 765 nm was composed using the same QWPs as above, but now used as HWPs at 765 nm. Representative transmittance spectra of two composite BB HWPs, assembled with three and five HWPs, are presented in Fig. 3. The transmittance spectrum of a single HWP at 765 nm is shown for comparison. The calculated retardance is shown in the inset in Fig. 3. As in Fig. 2, we find significant wavelength range broadening. As expected, the

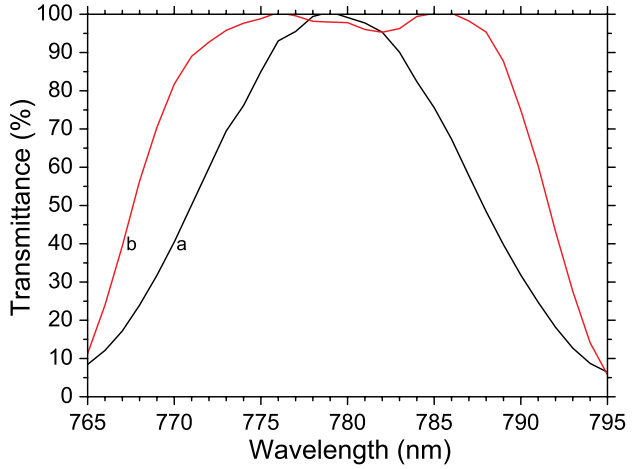

Fig. 2. Measured transmittance for the BB composite HWP formed of a sequence of QWPs: (a) Reference spectrum of an HWP made of two QWPs; (b) BB HWP retarder made of six QWPs with rotation angles 45.5°, 78.5°, 76.7°, 15.5°, 17.7°, and 45.4°.

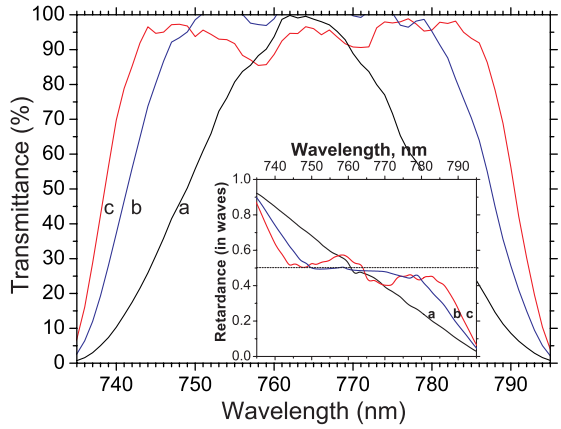

Fig. 3. Measured transmittance for the BB composite HWP assembled from a sequence of QWPs used as HWPs at 765 nm. (a) Reference spectrum of one QWP; (b) BB HWP retarder made of three QWPs with rotation angles 14.7°, 164.4°, and 14.7°; (c) BB HWP retarder made of five QWPs with rotation angles 7.5°, 172.5°, 14.2°, 172.9°, and 8.6°. The inset presents the retardance.

composite HWP with a higher number of constituent WPs has a wider wavelength range.

B. Composite Polarization Filters

Standard multiorder WPs are NB retarders. Using a proper set of rotation angles, a composite NB retarder can be assembled with a much narrower wavelength range. Here we demonstrate how with the same set of QWPs as used above, but rotated at different angles, an NB HWP can be assembled. Figure 4 shows representative transmittance curves for composite NB filters constructed of five and six QWPs, respectively. The six-plate composite NB filter reduces the width (at half-maximum) of the transmittance spectrum by a factor of almost 3. The comparison of the transmittance spectra (curves b and c) shows that the filter bandwidth is narrower for a higher number of WPs. Even with this limited number of WPs one can produce filters with a bandwidth of about 7 nm. There is no fundamental physical limit (except the divergence of the light beam) that can prevent us from going to as narrow a width of the transmission profile as we like.

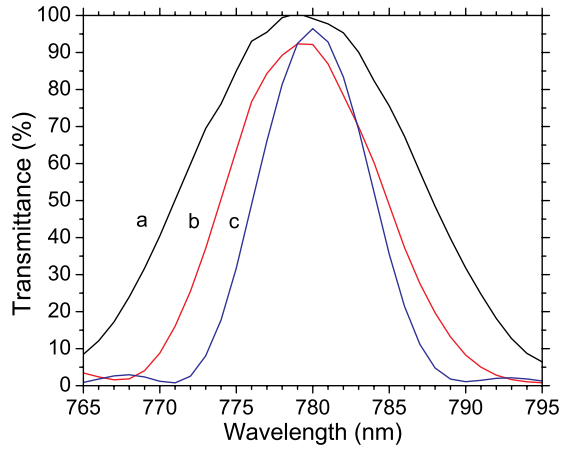

Fig. 4. Measured transmittance for NB composite filters. (a) Reference spectrum of two QWPs; (b) filter of five QWPs, with rotation angles (43.7°, 176.9°, 170.1°, 119.3°, 80.2°); (c) filter of six QWPs, with rotation angles 165.3°, 167°, 19.7°, 18.6°, 166.4°, and 166.1°.

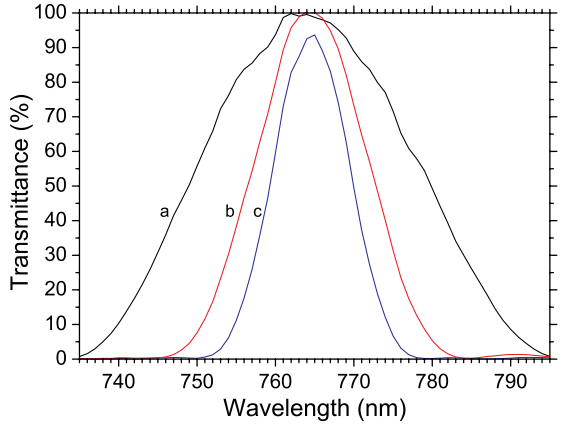

Fig. 5. Measured transmittance for composite filters. (a) Reference spectrum of one HWPs; (b) filter of three HWPs, with rotation angles 14.7°, 45.1°, and 75.3°; (c) filter of five HWPs, with rotation angles 37.7°, 83.1°, 49.9°, 1.9°, and 38.2°.

With sufficiently many WPs, one can reduce the bandwidth even below 1 nm for a sufficiently collimated light beam.

As for BB retarders, we have calculated sets of angles for the NB HWPs assembled using the QWPs as HWPs at 765 nm. The results are shown in Fig. 5. Again, a reduction of the transmittance bandwidth by a factor of 3 is established with the five-plate composite filter.

C. Tunable Composite Polarization Filters

As was already shown, very NB optical filters can be assembled using a stack of QWPs or HWPs with properly chosen rotation angles. Furthermore, the calculation method presented above can also be applied to solve the problem of making these filters tunable. The tunability was tested for a composite HWP filter composed of six QWPs. The measured set of transmittance spectra is shown in Fig. 6. It is seen that by properly choosing the rotation angles the filter's spectral band can be moved at will. Remarkably, the bandwidth of the transmittance curves does not change with the tuning

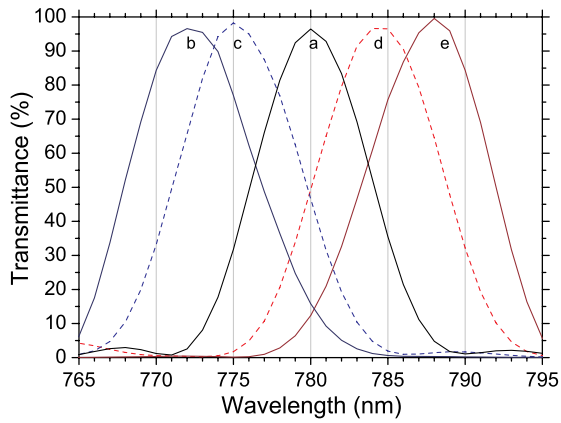

Fig. 6. Measured transmittance of composite filters made of the same set of six QWPs, but for different rotation angles. The central wavelength is tuned to the following: (a) 780 nm (design wavelength, no tuning, retardation $\varphi' = 0.50\pi$); (b) 772 nm ($\varphi' = 0.25\pi$); (c) 775 nm ($\varphi' = 0.35\pi$); (d) 784 nm ($\varphi' = 0.65\pi$); (e) 788 nm ($\varphi' = 0.75\pi$). The rotation angles are as follows: a, 165.3°, 167.1°, 19.7°, 18.6°, 166.4°, and 166.1°; b, 8.9°, 158.1°, 158.9°, 116.1°, 51.5°, and 34.5°; c, 26.4°, 154.7°, 178.6°, 1.3°, 20.2°, and 158.8°; d, 60.4°, 14.1°, 175.7°, 178.4°, 154.2°, and 110.6°; e, 6.2°, 25.4°, 50.2°, 56.1°, 39.0°, and 13.4°.

of the filter. In addition, one could use the multiorder WPs as QWPs or as HWPs at different wavelengths, as shown in the previous section, thus constructing tunable NB filters in a wide wavelength range.

5. CONCLUSION

We have demonstrated that by using a stack of ordinary (chromatic) multiorder WPs, which act as an HWP at 765 nm and a QWP at 780 nm, one can build efficient polarization BB (achromatic) half-wave composite retarders and tunable NB polarization filters. By rotating the same set of WPs at specific angles, we have constructed a BB HWP around 780 nm, a BB HWP around 765 nm, and a tunable HWP filter at several wavelengths from 765 to 788 nm. Better (broader) BB retarders can be built with lower-order WPs. Polarization filters with a narrower bandwidth (FWHM), even below 1 nm, can be constructed with sufficiently many high-order (the higher the better) WPs.

ACKNOWLEDGMENTS

This work was supported by the Bulgarian NSF Grant DRila-01/4 and the European Community's Seventh Framework Programme under grant agreement no. 270843 (iQIT).

REFERENCES

1. D. Grischkowsky, S. R. Keinding, M. van Exter, and C. Fattinger, "Far-infrared time-domain spectroscopy with terahertz beams of dielectrics and semiconductors," J. Opt. Soc. Am. B **7**, 2006–2015 (1990).
2. J.-B. Masson and G. Gallot, "Terahertz achromatic quarter-wave plate," Opt. Lett. **31**, 265–267 (2006).
3. S. Hanany, J. Hubmayr, B. R. Johnson, T. Matsumura, P. Oxley, and M. Thibodeau, "Millimeter-wave achromatic half-wave plate," Appl. Opt. **44**, 4666–4670 (2005).
4. G. Pisano, G. Savini, P. A. R. Ade, V. Hanes, and W. K. Gear, "Achromatic half-wave plate for submillimeter instruments in cosmic microwave background astronomy: experimental characterization," Appl. Opt. **45**, 6982–6989 (2006).
5. T. Matsumura, S. Hanany, P. A. R. Ade, B. R. Johnson, T. J. Jones, P. Jonnalagadda, and G. Savini, "Performance of three- and five-stack achromatic half-wave plates at millimeter wavelengths," Appl. Opt. **48**, 3614–3625 (2009).
6. C. D. West and A. S. Makas, "The spectral dispersion of birefringence, especially of birefringent plastic sheets," J. Opt. Soc. Am. **39**, 791–794 (1949).
7. M. G. Destriau and J. Prouteau, "Réalisation d'un quart d'onde quasi achromatique par juxtaposition de deux lames cristallines de même nature," J. Phys. Radium **10**, 53–55 (1949).
8. S. Pancharatnam, "Achromatic combinations of birefringent plates. Part I: an achromatic circular polarizer," Proc. Indian Acad. Sci. **41**, 130–136 (1955).
9. S. Pancharatnam, "Achromatic combinations of birefringent plates. Part II: an achromatic quarter-WP," Proc. Indian Acad. Sci. **41**, 137–144 (1955).
10. S. E. Harris, E. O. Ammann, and A. C. Chang, "Optical network synthesis using birefringent crystals. I. Synthesis of lossless networks of equal-length crystals," J. Opt. Soc. Am. A **54**, 1267–1279 (1964).
11. C. M. McIntyre and S. E. Harris, "Achromatic wave plates for the visible spectrum," J. Opt. Soc. Am. A **58**, 1575–1580 (1968).
12. Z. Zhuang, Y. J. Kim, and J. S. Patel, "Achromatic linear polarization rotator using twisted nematic liquid crystals," Appl. Phys. Lett. **76**, 3995–3997 (2000).
13. M. D. Lavrentovich, T. A. Sergan, and J. R. Kelly, "Switchable broadband achromatic half-wave plate with nematic liquid crystals," Opt. Lett. **29**, 1411–1413 (2004).
14. A. M. Title and W. J. Rosenberg, "Tunable birefringent filters," Opt. Eng. **20**, 815–823 (1981).
15. B. Lyot, "Filter monochromatique polarisant et ses applications en physique solaire," Ann. Astrophys. **7**, 31–79 (1944).
16. J. W. Evans, "Solc birefringent filter," J. Opt. Soc. Am. **48**, 142–145 (1958).
17. I. Šolc, "Birefringent chain filters," J. Opt. Soc. Am. **55**, 621–625 (1965).
18. J. M. Beckers, L. Dickson, and R. S. Joyce, "Observing the sun with a fully tunable Lyot-Ohman filter," Appl. Opt. **14**, 2061–2066 (1975).
19. G. A. Kopp, M. J. Derks, D. F. Elmore, D. M. Hassler, J. C. Woods, J. L. Streete, and J. G. Blankner, "Tunable liquid-crystal filter for solar imaging at the He i 1083-nm line," Appl. Opt. **36**, 291–296 (1997).
20. G. Shabtay, E. Eidinger, Z. Zalevsky, D. Mendlovic, and E. Marom, "Tunable birefringent filters—optimal iterative design," Opt. Express **10**, 1534–1541 (2002).
21. I. Abdulhalim, "Polarized optical filtering from general linearly twisted structures," Opt. Commun. **267**, 36–39 (2006).
22. I. Abdulhalim, "Effect of the number of sublayers on axial optics of anisotropic helical structures," Appl. Opt. **47**, 3002–3008 (2008).
23. O. Aharon and I. Abdulhalim, "Tunable optical filter having a large dynamic range," Opt. Lett. **34**, 2114–2116 (2009).
24. O. Aharon and I. Abdulhalim, "Liquid crystal Lyot tunable filter with extended free spectral range," Opt. Express **17**, 11426–11433 (2009).
25. G. D. Sharp, K. M. Johnson, and D. Doroski, "Continuously tunable smectic A^* liquid-crystal color filter," Opt. Lett. **15**, 523–525 (1990).
26. M. H. Levitt, "Composite pulses," Prog. Nucl. Magn. Reson. Spectrosc. **18**, 61–122 (1986).
27. H. Häffner, C. F. Roos, and R. Blatt, "Quantum computing with trapped ions," Phys. Rep. **469**, 155–203 (2008).
28. N. Timoney, V. Elman, S. Glaser, C. Weiss, M. Johanning, W. Neuhauser, and C. Wunderlich, "Error-resistant single-qubit gates with trapped ions," Phys. Rev. A **77**, 052334 (2008).
29. R. C. Jones, "A new calculus for the treatment of optical systems," J. Opt. Soc. Am. **31**, 488–493 (1941).
30. A. Ardavan, "Exploiting the Poincaré–Bloch symmetry to design high-fidelity broadband composite linear retarders," New J. Phys. **9**, 24 (2007).
31. S. Wimperis, "Broadband, narrowband, and passband composite pulses for use in advanced NMR experiments," J. Magn. Reson. **109**, 221–231 (1994).
32. S. S. Ivanov, A. A. Rangelov, N. V. Vitanov, T. Peters, and T. Halfmann, "Highly efficient broadband conversion of light polarization by composite retarders," J. Opt. Soc. Am. A **29**, 265–269 (2012).
33. T. Peters, S. S. Ivanov, D. Englisch, A. A. Rangelov, N. V. Vitanov, and T. Halfmann, "Variable ultra-broadband and narrowband composite polarization retarders," Appl. Opt. **51**, 7466–7474 (2012).